

# Characterization and Catalytic Performance of PtSn Catalysts Supported on Al<sub>2</sub>O<sub>3</sub> and Na-doped Al<sub>2</sub>O<sub>3</sub> in *n*-butane Dehydrogenation

Sergio R. de Miguel · Sonia A. Bocanegra ·  
I. M. Julieta Vilella · A. Guerrero-Ruiz ·  
Osvaldo A. Scelza

Received: 7 May 2007 / Accepted: 11 July 2007 / Published online: 25 July 2007  
© Springer Science+Business Media, LLC 2007

**Abstract** PtSn/Al<sub>2</sub>O<sub>3</sub> and PtSn/Al<sub>2</sub>O<sub>3</sub>–Na catalysts display important modifications of the metallic phase with respect to Pt/Al<sub>2</sub>O<sub>3</sub> one. In this sense, TPR and XPS results show the presence of strong interactions between Pt and Sn, with probable alloy formation, which would be responsible for the decrease of the reaction rate and the increase of the activation energy in cyclohexane dehydrogenation. Besides the experiments of cyclopentane hydrogenolysis show that the alkali metal addition to bimetallic PtSn/Al<sub>2</sub>O<sub>3</sub> catalysts completely eliminates the hydrogenolytic ensembles, which could be due to a geometric modification of the metallic phase. These important modifications in the nature of the metallic function due to the simultaneous addition of Na and Sn to Pt/Al<sub>2</sub>O<sub>3</sub> are responsible for the excellent catalytic performance in the *n*-butane dehydrogenation, thus giving high conversions, selectivities to butenes higher than 95%, and lower deactivation capacity than those corresponding to bimetallic PtSn catalysts (with different Sn contents) supported on undoped alumina. The excellent stability of PtSn/Al<sub>2</sub>O<sub>3</sub>–Na catalysts would be due to a low carbon formation during the reaction, such as it was observed from pulse experiments.

**Keywords** Paraffin dehydrogenation · Pt and PtSn supported catalysts · Na-doped alumina supports · Characterization of supported metallic catalysts

## 1 Introduction

Bimetallic catalysts supported on alumina are active for naphtha reforming and dehydrogenation of paraffins of both low and high molecular weight. [1–6]. One important difference between naphtha reforming and dehydrogenation catalysts is related to their acidic character. Thus, for the reforming of hydrocarbons it is required a given acidity level to obtain an adequate balance between the metallic and the acidic function, which gives the bifunctional character [7]. In the case of the dehydrogenation catalysts, the side reactions (cracking, isomerization and polymerization), which are catalyzed by acidic centers, should be inhibited and thus the yield to the corresponding olefins increases. In order to minimize the undesirable side reactions, the acidic sites of the support can be poisoned by the addition of alkali metal ions during the preparation of the catalysts. It must be indicated that several studies on this topic have been reported in the literature. Thus, Pines and Haag [8] found that alkali metal ions poison the Lewis acidic sites of the alumina. Jiratová and Beranek [9] reported a selective poisoning of the support when alumina is doped with Na ions. García Cortez et al. [10] and Bocanegra et al. [11], found that Li, Na and K ions poison the acidic sites of alumina. Moreover, these authors reported that the strong acidic sites are poisoned by the addition of small quantities of alkali metal ions. Further addition of these ions appears to block centers with lower acidic strength. Likewise, it was also found [10] that the toxicity of the alkali metals on the acidic character of

S. R. de Miguel (✉) · S. A. Bocanegra ·  
I. M. J. Vilella · O. A. Scelza  
Instituto de Investigaciones en Catálisis y Petroquímica,  
Facultad de Ingeniería Química, Universidad Nacional del  
Litoral-CONICET, Santiago del Estero 2654, Santa Fe 3000,  
Argentina  
e-mail: sdmiguel@fiqus.unl.edu.ar

A. Guerrero-Ruiz  
Facultad de Ciencias, Universidad Nacional de Educación a  
Distancia, Madrid, Spain

alumina increases with the ionic radius, though the poisoning effect of Na, K and Li would not be related only to a steric effect. Besides, de Miguel et al. [12] found, through FTIR of pre-adsorbed CO and NMR measurements, that K and Li are selectively adsorbed on tetrahedrally coordinated Lewis  $\text{Al}^{3+}$  sites of the alumina surface, this effect being more pronounced for K. However, the addition of alkali metals to alumina not only modifies the acidic function, but also it affects the structure of the metallic phase. In fact, Mross [13] reported that the alkali metals could change the electronic structure of the transition metals and, in consequence, the activity in the CO hydrogenation reaction is enhanced. Park and Price [14, 15] reported that K addition to Pd/ $\text{Al}_2\text{O}_3$  catalyst increases both the activity and the selectivity in the acetylene hydrogenation. This behavior was explained in terms of the increase of the support basicity, and an electronic transference from K to Pd. Rodríguez et al. [16] reported that the addition of potassium to Pt–Sn/ $\text{SiO}_2$  did not change the activity of the fresh catalysts in the isobutane dehydrogenation reaction, but it improved the dehydrogenation selectivity, which reached values of almost 100%. Besides, Vernoux et al. [17] found for the selective catalytic reduction (SCR) of  $\text{NO}_x$  by propene and propane under lean-burn conditions, that the addition of Na markedly modified the Pt catalytic behavior.

In this paper, a complete characterization of both acidic and metallic phases of PtSn/ $\text{Al}_2\text{O}_3$  catalyst and PtSn/ $\text{Al}_2\text{O}_3$ –Na catalysts is carried out by using isopropanol dehydration, X-ray Photoelectron Spectroscopy (XPS), Temperature Programmed Reduction (TPR) and test reactions of the metallic phase. Besides the influence of the Na addition to PtSn/ $\text{Al}_2\text{O}_3$  on the activity, selectivity and deactivation (by coke formation) in the *n*-butane dehydrogenation reaction is analyzed by using flow and pulse reactors.

## 2 Experimental

Catalysts were prepared by using a commercial  $\gamma$ - $\text{Al}_2\text{O}_3$  (CK-300 from Cyanamid Ketjen,  $S_{\text{BET}} = 180 \text{ m}^2 \text{ g}^{-1}$ ) previously calcined in flowing air at 650 °C for 3 h. The alumina samples doped with Na in different concentrations (0.05, 0.15, 0.25 and 0.5 wt%) were obtained by impregnating the support with an aqueous solution of NaOH, using a volume of solution/weight of support ratio of 1.4 mL  $\text{g}^{-1}$  and a NaOH concentration such as to obtain the desired Na loading on the support. PtSn/ $\text{Al}_2\text{O}_3$ –Na (0.5 wt%) catalysts were prepared by an initial impregnation with NaOH. Then, Pt and Sn were incorporated either by successive impregnation or coimpregnation. In the first case, Pt was deposited from an aqueous solution of  $\text{H}_2\text{PtCl}_6$  (0.011 M), dried at 120 °C for 12 h, and then the samples

were impregnated with a hydrochloric solution of  $\text{SnCl}_2$ . In the case of coimpregnation, both metallic precursors were simultaneously added to the impregnating solution. The impregnation volume/support weight ratio was 1.4 mL  $\text{g}^{-1}$  in all cases. After the impregnation, samples were dried at 120 °C. The metallic contents were 0.3 wt% for Pt, and 0.3 or 0.5 wt% for Sn. After impregnation, samples were dried at 120 °C and finally calcined at 500 °C in flowing air for 3 h. Moreover, the monometallic Pt (0.3 wt%)/ $\text{Al}_2\text{O}_3$  catalyst was prepared by alumina impregnation with an aqueous solution of  $\text{H}_2\text{PtCl}_6$ .

The acidic properties of pure and Na-doped alumina samples were determined by isopropanol (IPA) dehydration reaction at 250 °C and atmospheric pressure in a flow reactor, using a  $\text{H}_2$ /IPA molar ratio of 18 and a space velocity of 32  $\text{h}^{-1}$ .

The textural properties of  $\text{Al}_2\text{O}_3$  and  $\text{Al}_2\text{O}_3$ –Na were determined in a Quantachrome Corporation NOVA 1000 surface area analyzer. It was observed that the specific textural properties (specific surface area and pore size distribution) of the support are practically unmodified by the alkali metal addition between 0 and 0.5 wt% Na.

Two different *n*-butane dehydrogenation tests were carried out, one of them in a continuous flow reactor and the other one in a pulse equipment. The continuous flow experiments were performed at 530 °C for 2 h in a quartz flow reactor heated by an electric furnace. The reactor (with a catalyst weight of 0.200 g) was fed with 18 mL  $\text{min}^{-1}$  of the reactive mixture (*n*-butane + hydrogen,  $\text{H}_2/n\text{-C}_4\text{H}_{10}$  molar ratio = 1.25). The reactive mixture was prepared “in situ” by using mass flow controllers. All gases, *n*-butane,  $\text{N}_2$  (used for purge), and  $\text{H}_2$  (used for the previous reduction of catalysts and for the reaction) were high purity ones (>99.99%). Prior to the reaction, catalysts were reduced “in situ” at 530 °C under flowing  $\text{H}_2$  for 3 h. The reactor effluent was analyzed in a GC-FID equipment with a packed chromatographic column (1/8” OD  $\times$  6 m, 20% BMEA on Chromosorb P-AW 60/80). The column was kept at 50 °C during the analysis and in this way, the amounts of methane, ethane, ethylene, propane, propylene, *n*-butane, 1-butene, *cis*-2-butene, *trans*-2-butene and 1,3 butadiene were measured. The *n*-butane conversion was calculated as the sum of the percentages of the chromatographic areas of the reaction products (except  $\text{H}_2$ ) corrected by the corresponding response factor. The selectivity to the different reaction products was defined as the ratio: mol of product *i* /  $\sum$  mol of all products (except  $\text{H}_2$ ). Taking into account the high temperatures used for the reaction (for thermodynamic reasons), it was necessary to determine the contribution of the homogeneous reaction. For this purpose, a blank experiment was performed by using a quartz bed and the results showed a negligible *n*-butane conversion (<<1%).

Pulse experiments were performed in order to determine the behavior of catalysts in the first steps of the reaction since the initial catalytic properties cannot be determined in flow experiments. These experiments were carried out by injecting pulses of pure *n*-butane (0.5 mL STP) into the catalytic bed (0.100 g of sample) at 530 °C. The catalytic bed was kept under flowing He (30 mL min<sup>-1</sup>) between the injection of two successive pulses. Prior to the experiments, all samples were reduced “in situ” under flowing H<sub>2</sub> at 530 °C for 3 h. The composition of each pulse after the reaction was determined by using a GC-FID equipment with a packed column (Porapak Q). The temperature of the chromatographic column was 30 °C. In these experiments the *n*-butane conversion was calculated as the difference between the chromatographic area of *n*-butane fed to the reactor (previously determined) and the chromatographic area of non-reacted *n*-butane at the outlet of the reactor, and this difference was referred to the chromatographic area of *n*-butane fed to the reactor. The selectivity to a given product was calculated in the same way as for flow experiments. The carbon amount retained by the catalyst after the injection of each pulse was calculated through a mass balance between the total carbon amount fed to the reactor and the total carbon amount detected by the chromatographic analysis at the outlet of the reactor. The accumulative carbon retention was calculated as the sum of the carbon amount retained after each pulse.

The characteristics of the metallic catalysts were determined by different techniques: test reactions of the metallic phase (cyclohexane dehydrogenation and cyclopentane hydrogenolysis), temperature programmed reduction (TPR) and X-ray photoelectron spectroscopy (XPS).

Test reactions of the metallic phase were performed in a differential flow reactor at atmospheric pressure. Cyclohexane (CH) dehydrogenation was carried out at 300 °C, by using a H<sub>2</sub>/CH molar ratio of 29 and a CH flow rate of 6 mL h<sup>-1</sup>. Prior to the reaction, catalysts were reduced at 500 °C. The activation energy in CH dehydrogenation for different catalysts was obtained by measuring the initial reaction rate at 270, 285 and 300 °C. Cyclopentane (CP) hydrogenolysis was done at 300 °C, H<sub>2</sub>/CP molar ratio = 25 and volumetric CP flow = 6 mL h<sup>-1</sup>. Prior to this reaction, catalysts were reduced at 500 °C. The sample weight used in these experiments was the appropriate to obtain a CH or CP conversion lower than 7%. The reaction products were only benzene and *n*-pentane for the first and second reaction, respectively. In both cases, the reaction products were analyzed by using a gas chromatographic system (packed column with Chromosorb and FID detector).

TPR experiments were performed in a quartz flow reactor. The samples were heated at 6 °C min<sup>-1</sup> from room temperature up to 800 °C. The reductive mixture (5% v/v H<sub>2</sub>-N<sub>2</sub>) was fed to the reactor with a flow rate of 10 mL

min<sup>-1</sup>. Catalysts were previously calcined “in situ” at 500 °C for 3 h.

XPS measurements were carried out in a VG-Microtech Multilab spectrometer, which operates with an energy power of 50 eV (radiation MgK $\alpha$ ,  $h\nu = 1253.6$  eV). The pressure of the analysis chamber was kept at  $4 \times 10^{10}$  torr. Samples were previously reduced “in situ” at 500 °C with H<sub>2</sub> for 2 h. Binding energies (BE) were referred to the C1s peak at 284.9 eV. The peak areas were determined by fitting the experimental results with Lorentzian–Gaussian curves.

### 3 Results and Discussion

#### 3.1 Isopropanol Dehydration

The poisoning effect of the Na addition on the acidic properties of the alumina was studied by means of the dehydration of isopropanol (IPA) to propylene (P) and di-isopropylether (E). Table 1 shows that the isopropanol conversion decreases as the amount of Na increases. It can also be observed that very low amounts of Na (0.25 wt%) added to Al<sub>2</sub>O<sub>3</sub> produce a strong inhibition of the dehydrating capacity, the activity being null for 0.5 wt% Na. The selectivity to di-isopropylether displays an analogous behavior since it decreases with the increase of the Na content, such as Table 1 shows. Taking into account that the ether formation would require strong acidic sites [10], the results obtained in the isopropanol dehydration would be in agreement with the high poisoning capacity of Na on the stronger acidic sites of the alumina. By considering these results, a Na content of 0.5 wt% was used for the preparation of the different Pt/Al<sub>2</sub>O<sub>3</sub>-Na and PtSn/Al<sub>2</sub>O<sub>3</sub>-Na catalysts.

#### 3.2 CH Dehydrogenation and CP Hydrogenolysis

Both test reactions of the metallic phase (CH dehydrogenation and CP hydrogenolysis) were carried out at 300 °C and the results are displayed in Table 2. This Table shows

**Table 1** Isopropanol (IPA) conversion and selectivity to di-isopropylether (E) (conversion to di-isopropylether  $\times$  100/conversion to propylene) as a function of the Na content added to alumina

| Na (wt%) added to Al <sub>2</sub> O <sub>3</sub> | IPA conversion (%) | Selectivity to E (%) |
|--|--------------------|----------------------|
| 0  | 65                 | 41                   |
| 0,05   | 22                 | 39                   |
| 0,15   | 9                  | 21                   |
| 0,25   | 2                  | 11                   |
| 0,5  | 0                  | –                    |

the initial reaction rates ( $R_{CH}$ ) and the activation energy values ( $E_{CH}$ ) for CH dehydrogenation, and the initial reaction rates ( $R_{CP}$ ) for CP hydrogenolysis. Besides, Table 2 displays a catalytic comparison between the behavior of bimetallic PtSn and monometallic Pt catalysts supported on  $Al_2O_3$  and  $Al_2O_3-Na$ .

For CH dehydrogenation, a structure-insensitive reaction [18], bimetallic PtSn catalysts show a decrease of the activity and an increase of the activation energy with respect to the corresponding supported monometallic catalysts. These effects are more pronounced for the bimetallic catalysts with the highest Sn content. These behaviors can be related to a certain electronic interaction between Pt and Sn, with probable alloy formation for the two bimetallic catalyst series, supported on alumina and Na-doped alumina. It must be noted that the increase of the activation energy is more pronounced for PtSn catalysts supported on alumina than for the ones supported on Na-doped alumina.

In the case of CP hydrogenolysis, a structure-sensitive reaction [19], a negligible activity is observed for the different bimetallic catalysts supported on alumina and Na-doped alumina (except for the PtSn(0.3 wt%)/ $Al_2O_3$  sample either SI or C which shows a very low activity). This indicates that Sn together with Na also produces a geometric modification of the metallic phase and therefore, the concentration of the metallic ensembles necessary for the hydrogenolysis reaction is practically suppressed.

The addition of Pt and Sn by using different impregnation sequences, such as coimpregnation or successive impregnation, appears to have a minor effect in both reactions.

### 3.3 Temperature Programmed Reduction (TPR)

Figure 1 shows the TPR profiles of bimetallic Pt(0.5 wt%)/Sn(0.15; 0.30 and 0.50 wt%)/ $Al_2O_3$  catalysts, prepared by successive impregnation, compared with the

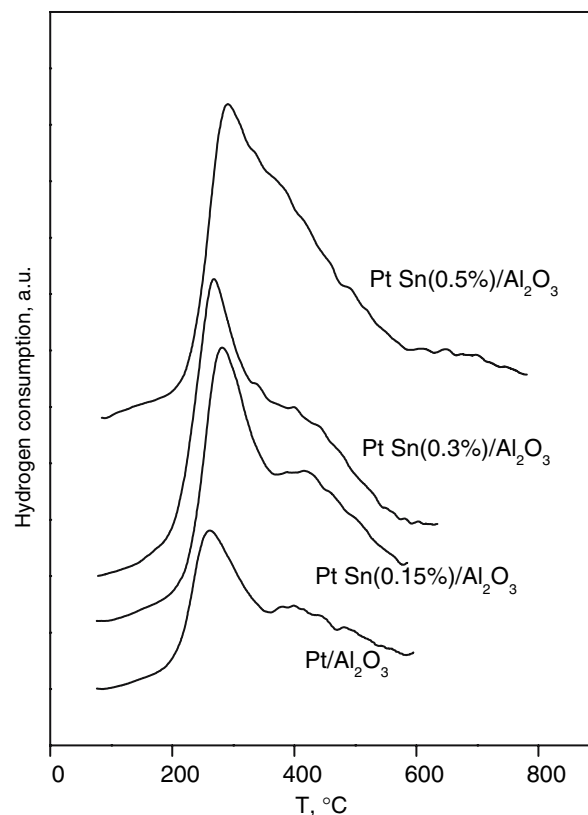


**Fig. 1** TPR profiles of Pt and PtSn/ $Al_2O_3$  catalysts prepared by successive impregnation

monometallic Pt/ $Al_2O_3$  sample. The TPR profile of the monometallic Pt/ $Al_2O_3$  catalyst shows a main reduction peak at 270 °C and a secondary reduction zone at 430 °C. The presence of these two reduction peaks is explained by the existence of two different oxychlorinated Pt species originated after the impregnation of the support with chloroplatinic acid and the subsequent thermal treatments (drying and calcination steps) [20, 21]. Lieske et al. [20]

**Table 2** Initial rates ( $R_{CH}$ ) and Activation energies ( $E_{CH}$ ) for the cyclohexane dehydrogenation at 300 °C, and initial rates ( $R_{CP}$ ) of cyclopentane hydrogenolysis at 300 °C for Pt/ $Al_2O_3$ , Pt/ $Al_2O_3-Na$  and PtSn/ $Al_2O_3-Na$  prepared by co-impregnation (C) and successive impregnation (SI)

| Catalyst                          | $R_{CH}$ (mol/h gPt) $T = 300$ °C | $E_{CH}$ (Kcal/mol) | $R_{CP}$ (mol/h g) $T = 300$ °C |
|-----------------------------------|-----------------------------------|---------------------|---------------------------------|
| Pt/ $Al_2O_3$                     | 108                               | 23                  | 2.4                             |
| PtSn(0.3 wt%)/ $Al_2O_3$ (C)      | 50                                | 28                  | 0.4                             |
| PtSn(0.3 wt %)/ $Al_2O_3$ (SI)    | 58                                | 29                  | 0.3                             |
| PtSn(0.5 wt %)/ $Al_2O_3$ (C)     | 30                                | 32                  | negligible                      |
| PtSn(0.5 wt %)/ $Al_2O_3$ (SI)    | 29                                | 33                  | negligible                      |
| Pt/ $Al_2O_3-Na$                  | 82                                | 23                  | 1.2                             |
| PtSn(0.3 wt %)/ $Al_2O_3-Na$ (C)  | 39                                | 25                  | negligible                      |
| PtSn(0.3 wt %)/ $Al_2O_3-Na$ (SI) | 46                                | 25                  | negligible                      |
| PtSn(0.5 wt %)/ $Al_2O_3-Na$ (C)  | 17                                | 26                  | negligible                      |
| PtSn(0.5 wt %)/ $Al_2O_3-Na$ (SI) | 28                                | 28                  | negligible                      |

studied Pt/ $\gamma$ -Al<sub>2</sub>O<sub>3</sub> catalysts treated at different temperatures in oxygen or hydrogen by temperature-programmed reduction and by hydrogen adsorption, and they found two chloride-containing surface complexes, [Pt<sup>IV</sup>(OH)<sub>x</sub>Cl<sub>y</sub>]<sub>s</sub> and [Pt<sup>IV</sup>O<sub>x</sub>Cl<sub>y</sub>]<sub>s</sub>. The formation of different oxidized Pt surface species was confirmed by characteristic uv–vis spectra by Lietz et al. [21]. The TPR profile of the Sn/Al<sub>2</sub>O<sub>3</sub> catalyst shows a reduction zone at high temperatures (500 °C), such as it was previously reported [22]. When Sn is added to the Pt/Al<sub>2</sub>O<sub>3</sub> catalyst, the first reduction peak is broader and shifted to higher temperatures. In this way, for the catalyst with the highest tin content (0.5 wt%), there is only a very wide peak appearing at 300 °C. It is important to note that there are not defined reduction signals in the temperature zone where Sn is reduced in the Sn/Al<sub>2</sub>O<sub>3</sub> catalyst. It should also be noted that there are not important differences between the TPR profiles of the co-impregnated and successively impregnated PtSn catalysts, thus indicating the presence of similar metallic phases in both catalysts. The increase of the magnitude of the peak at lower temperature, its broadening with the tin addition and the absence of reduction signals corresponding to segregated Sn, would indicate a simultaneous reduction or co-reduction of both metals, with probable formation of alloys or intermetallic compounds, in agreement with results reported in bibliography for PtSn/Al<sub>2</sub>O<sub>3</sub> catalysts and other bimetallic systems [23–26].

TPR profiles of bimetallic PtSn catalysts (with different Sn contents and different impregnation sequences) and monometallic Pt catalyst supported on Na-doped alumina are shown in Fig. 2. The comparison of the TPR profiles between Pt/Al<sub>2</sub>O<sub>3</sub>–Na (0.5 wt%) catalyst, and the undoped Pt/Al<sub>2</sub>O<sub>3</sub> one (Fig. 1) indicates that the first reduction peak is maintained at similar temperatures (270 °C) in both catalysts. However the second reduction peak is shifted to higher temperatures in Pt/Al<sub>2</sub>O<sub>3</sub>–Na catalysts (with a maximum at approximately 500 °C) with respect to that of Pt/Al<sub>2</sub>O<sub>3</sub> catalyst, and its intensity sharply increases. This behavior could be attributed to the formation of new species related with Na, such as it was observed by Bocanegra et al. [11], which would be reduced at lower temperature by hydrogen activated in the metallic Pt particles. In this sense, C.-H. Lee and Y.-W. Chen [27] reported for the Al<sub>2</sub>O<sub>3</sub>–Na sample, a main TPR peak at approximately 530 °C, due to the reduction of oxidized Na species. For the Pt/Al<sub>2</sub>O<sub>3</sub>–Na catalyst, the TPR profile displayed only one peak at 200 °C, which could be assigned to the reduction of Pt oxide and oxygen shared with Na. The authors concluded that there might be a hydrogen spillover phenomenon on Pt supported on alkali metal doped Al<sub>2</sub>O<sub>3</sub> during the TPR process in which hydrogen adsorbed on a Pt atom migrates to Na<sub>2</sub>O in close proximity to Pt. Besides, Rodriguez et al. [28] reported in the TPR profile of Pt/SiO<sub>2</sub>–K a peak at 410 °C, assigned to the

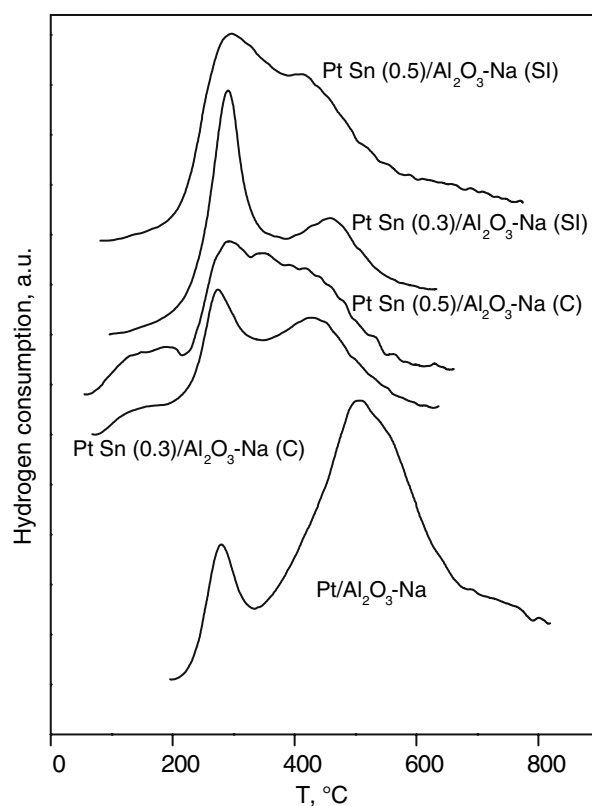


Fig. 2 TPR profiles of Pt and PtSn/Al<sub>2</sub>O<sub>3</sub>–Na catalysts

reduction of KO<sub>x</sub> species by hydrogen activated in the Pt(0) particles.

By comparing the TPR profiles of bimetallic catalysts supported on Na-doped alumina prepared by different impregnation sequences, there are no important qualitative differences attributed to the preparation procedure, but there are differences among the catalysts with different Sn contents. Thus, PtSn/Al<sub>2</sub>O<sub>3</sub>–Na catalysts with 0.3 wt% Sn (Fig. 2) show two well-defined reduction peaks, the former being larger and appearing at low temperature (280–300 °C), and the latter being smaller and appearing at high temperature (430–470 °C). On the other hand, PtSn/Al<sub>2</sub>O<sub>3</sub>–Na catalysts with 0.5 wt% Sn display a wide reduction zone between 200 °C and 500 °C, with a maximum at 300 °C.

The reduction zone at low temperatures could correspond to strong interactions between Pt and Sn in agreement with the CH dehydrogenation results. Besides, these bimetallic catalysts supported on Na-doped alumina do not show the important reduction peak at 500 °C that Pt/Al<sub>2</sub>O<sub>3</sub>–Na catalysts do because of the reduction of new species related with Na [11, 27, 28]. The absence of this TPR peak at 500 °C in the PtSn/Al<sub>2</sub>O<sub>3</sub>–Na catalyst could be attributed to the presence of strong PtSn interactions that do not catalyze the reduction of the new species related with Na, such as free Pt<sup>0</sup> species do.

### 3.4 X-ray Photoelectron Spectroscopy (XPS)

XPS spectra of the Pt 4f level for the PtSn(0.5 wt%)/Al<sub>2</sub>O<sub>3</sub>, PtSn(0.5 wt%)/Al<sub>2</sub>O<sub>3</sub>-Na(0.5 wt%) (C) and PtSn(0.5 wt%)/Al<sub>2</sub>O<sub>3</sub>-Na(0.5 wt%) (SI) catalysts, reduced “in situ” at 500 °C, are presented in Fig. 3. Taking into account that the Pt 4f peaks overlaps with the Al 2p peaks of the alumina, a procedure of curve synthesis was performed assuming a Pt4f<sub>7/2</sub> to Pt4f<sub>5/2</sub> intensity ratio of 1:0.75. Table 3 compiles Pt4f<sub>7/2</sub> and Sn3d<sub>5/2</sub> binding energies

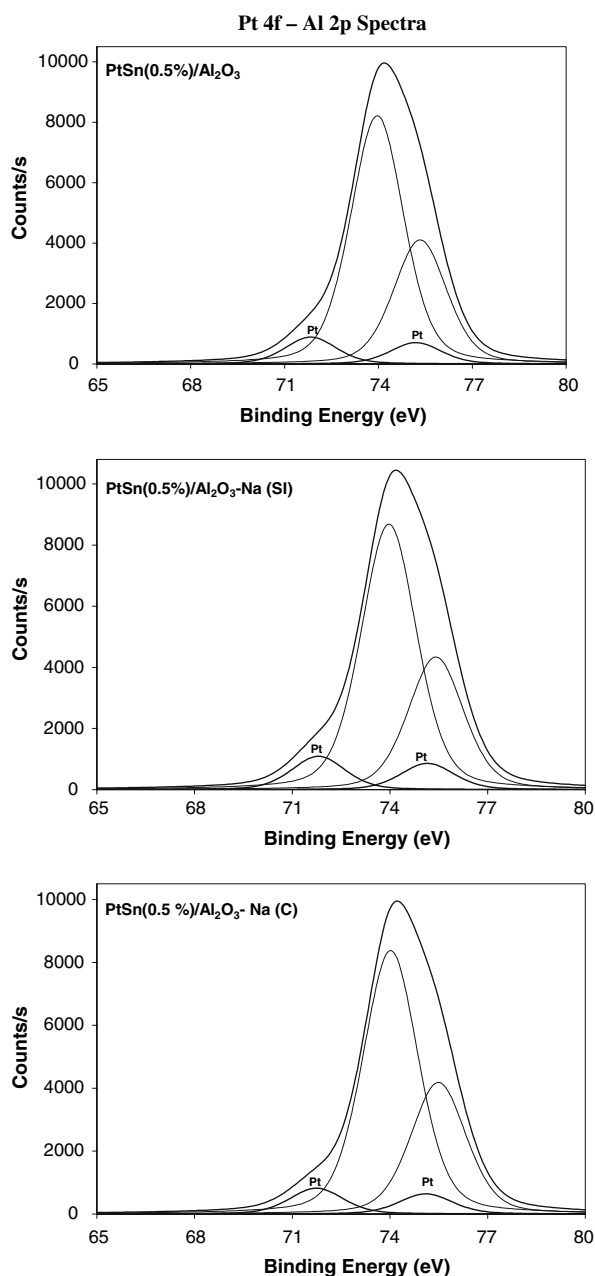


**Fig. 3** XPS spectra corresponding to Pt4f and Al2p signals of PtSn catalysts supported on Al<sub>2</sub>O<sub>3</sub> and Al<sub>2</sub>O<sub>3</sub>-Na

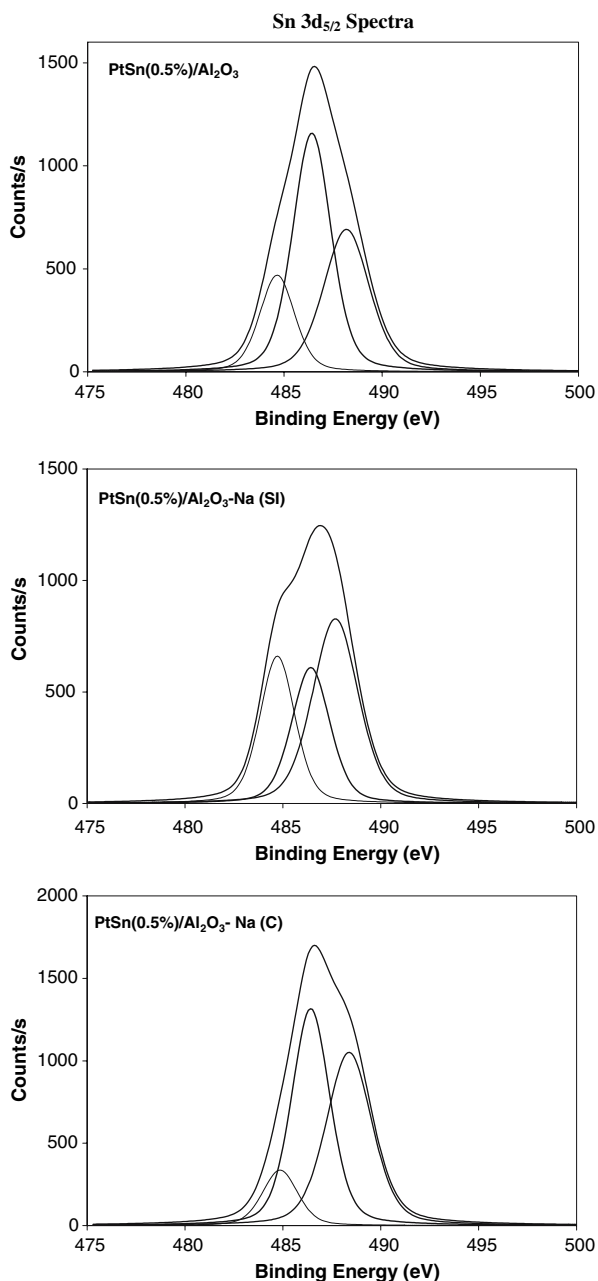
corresponding to the three bimetallic catalysts supported on alumina and Na(0.5 wt%)-doped alumina. The binding energy of Pt 4f<sub>7/2</sub> indicates in all cases only the presence of surface Pt<sup>0</sup> species.

Figure 4 shows the XPS spectra corresponding to the Sn 3d<sub>5/2</sub> level of PtSn(0.5 wt%)/Al<sub>2</sub>O<sub>3</sub>, PtSn(0.5 wt%)/Al<sub>2</sub>O<sub>3</sub>-Na (C) and PtSn(0.5 wt%)/Al<sub>2</sub>O<sub>3</sub>-Na (SI) catalysts after “in situ” reduction at 500 °C. From the deconvolution of the spectrum of the PtSn(0.5 wt%)/Al<sub>2</sub>O<sub>3</sub> catalyst, three peaks were obtained at 484.8, 486.5 and 488.2 eV. The first peak corresponds to zerovalent Sn, in agreement with results found by several authors [29–31]. It must be noted that Homs et al. [32] attributed the peaks at 483.6 eV and 485 eV to Sn(0) and Sn in a PtSn alloy (Sn<sup>0</sup><sub>al</sub>), respectively. The other two peaks appearing at 486.5 eV and 488.2 eV, would correspond to different types of oxidized Sn. According to the literature, the line corresponding to Sn 3d<sub>5/2</sub> for SnO has a BE at 486.5–486.8 eV, while the Sn 3d<sub>5/2</sub> line for SnO<sub>2</sub> has a BE at 486.5 eV [29–33], therefore it is not possible to discriminate the oxidation state of Sn corresponding to the signal positioned at 486.5 eV. In consequence, the second peak will be assigned to Sn(II)/Sn(IV) oxides. Besides, the third peak appearing at 488.2 eV could be probably due to chlorinated tin species bounded to the support [34–36]. From the deconvolution of the Sn 3d<sub>5/2</sub> line of the spectrum corresponding to the PtSn(0.5 wt%)/Al<sub>2</sub>O<sub>3</sub>-Na(0.5 wt%) (C) and PtSn(0.5 wt%)/Al<sub>2</sub>O<sub>3</sub>-Na(0.5 wt%) (SI) catalysts, three peaks were also obtained at 484.7 eV, 486.5 eV and 488.4 eV for the first one and at 484.7, 486.5 and 487.7 eV for the last one. As it was concluded for the bimetallic catalyst supported on undoped alumina, the first XPS peak would correspond to zerovalent Sn, while the second and the third peaks would be due to Sn(II)/Sn(IV) oxides and to chlorinated tin species bounded to the support, respectively.

Table 3 also shows Pt/Al, Sn/Al and Sn/Pt surface atomic ratios. The presence of Sn(0) in bimetallic catalysts (variable between 12% and 27% for the three catalysts) and the absence of this species in the Sn monometallic one, would indicate a higher Sn reducibility in PtSn catalysts, these results agreeing with TPR ones. Taking into account the above mentioned results for reduced bimetallic catalysts, it can be concluded that in these catalysts supported both on undoped and Na-doped alumina, a fraction of Sn would be as Sn(0), probably alloyed with Pt, and the remaining Sn would be as Sn(II)/Sn(IV) oxides and there would also be chlorinated tin species bounded to the support. Besides, from the XPS results it was determined the Sn/Pt surface atomic ratios, which were lower than the bulk Sn/Pt atomic ratio of the catalysts (2.74). Hence, it can be inferred that there is not any surface enrichment in Sn for both catalyst series (Na-doped Al<sub>2</sub>O<sub>3</sub> and Al<sub>2</sub>O<sub>3</sub>). This

**Table 3** Catalysts characterization by XPS. The values between parentheses indicate the percentage of each species

| Catalyst  | BE Pt 4f <sub>7/2</sub> (eV) | BE Sn 3d <sub>5/2</sub> (eV)          | Pt/Al  | Sn/Al  | Sn/Pt |
|---|------------------------------|---------------------------------------|--------|--------|-------|
| PtSn(0.5 wt%)/Al <sub>2</sub> O <sub>3</sub> (C)      | 71.8 (100%)                  | 484.7 (18%), 486.4 (48%), 488.2 (34%) | 0.0050 | 0.0097 | 1.92  |
| PtSn(0.5 wt%)/Al <sub>2</sub> O <sub>3</sub> -Na (C)  | 71.7 (100%)                  | 484.9 (12%), 486.5 (45%), 488.4 (43%) | 0.0046 | 0.0114 | 2.49  |
| PtSn(0.5 wt%)/Al <sub>2</sub> O <sub>3</sub> -Na (SI) | 71.7 (100%)                  | 484.8 (27%), 486.5 (28%), 487.7 (45%) | 0.0059 | 0.0084 | 1.43  |

**Fig. 4** XPS spectra corresponding to Sn3d<sub>5/2</sub> signals of PtSn catalysts supported on Al<sub>2</sub>O<sub>3</sub> and Al<sub>2</sub>O<sub>3</sub>-Na

agree with the XPS studies reported by Balakrishnan and Schwank [37] who inferred that except for very high Sn/Pt atomic ratios (1.0 Pt 5.0 Sn/Al<sub>2</sub>O<sub>3</sub> catalyst), the other

catalysts with lower Sn/Pt atomic ratios did not show enrichment of tin on the surface. Other authors found a certain Sn surface enrichment in Pt Sn catalysts supported on other materials such as SiO<sub>2</sub> [32], ZnAl<sub>2</sub>O<sub>4</sub> and MgAl<sub>2</sub>O<sub>4</sub> [36] and activated carbons [38].

### 3.5 Reaction of *n*-butane Dehydrogenation

Table 4 shows the initial ( $X_0$ , at 10 min of the reaction time) and final ( $X_f$ , at 120 min of the reaction time) values of the *n*-butane conversions in flow experiments for mono Pt and bimetallic PtSn catalysts supported on Al<sub>2</sub>O<sub>3</sub> and Al<sub>2</sub>O<sub>3</sub>-Na. Besides, the values corresponding to the deactivation parameter ( $D$ ) along the reaction time, which is defined as:  $[(X_0 - X_f) \cdot 100 / X_0]$ , are also included in this Table. It should be noted that alumina and Na doped alumina are inactive for this reaction at 530 °C.

It can be observed that the Pt/Al<sub>2</sub>O<sub>3</sub> catalyst has a high initial conversion, but it deactivates quickly after 2 h of reaction time ( $D = 78\%$ ). Tin addition to Pt/Al<sub>2</sub>O<sub>3</sub> catalyst without Na produces a small decrease both in the initial conversion and deactivation parameter ( $D$ ). The lowest value of  $D$  (58%) corresponds to the bimetallic catalyst with the highest Sn content (0.5 wt%).

Table 4 also shows the initial ( $S_0$ ) and final ( $S_f$ ) values of the selectivity to all butenes (1-butene, cis- and trans-2-butenes, and 1–3 butadiene) for the different catalysts. The dehydrogenating selectivity to all butenes of Pt/Al<sub>2</sub>O<sub>3</sub> catalyst is very low ( $\approx 60\%$ ) since the hydrogenolysis reactions, which produce light gases such as methane, ethane, ethylene, propane and propylene, are very important. Besides, it can be observed in Table 4 that the tin addition to Pt/Al<sub>2</sub>O<sub>3</sub> catalyst produces an important increase of the selectivity to butanes reaching values of 78–83%. This important increase of the dehydrogenation selectivity goes parallel to a pronounced decrease of the hydrogenolytic activity.

In conclusion, it could be observed from the reaction experiments in a flow system that the Sn addition to Pt/Al<sub>2</sub>O<sub>3</sub> catalyst decreases the deactivation rate of the catalyst along the reaction time (2 h), and favors the selectivity to butenes.

In order to understand the reasons of the better catalytic behavior of the bimetallic PtSn catalysts with respect to the Pt/Al<sub>2</sub>O<sub>3</sub> one, pulse experiments were carried out to study with more detail the initial steps of the *n*-butane

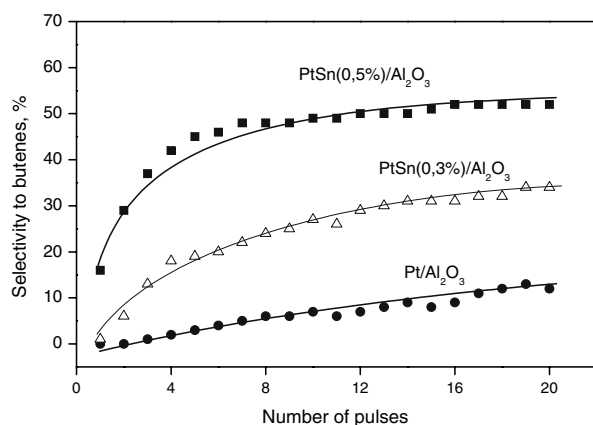
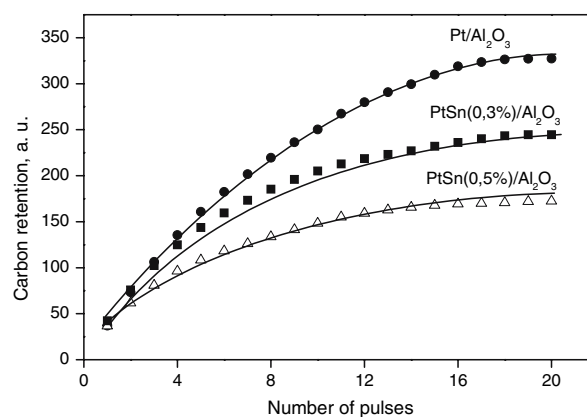
**Table 4** Activity and selectivity values for different catalysts in *n*-butane dehydrogenation at 530 °C. The Na content in all catalysts was 0.5 wt%

| Catalyst  | X <sub>0</sub> (%) | X <sub>f</sub> (%) | D (%) | S <sub>0</sub> (%) | S <sub>f</sub> (%) |
|---|--------------------|--------------------|-------|--------------------|--------------------|
| Pt/Al <sub>2</sub> O <sub>3</sub>                     | 45                 | 10                 | 78    | 64                 | 56                 |
| PtSn(0.3 wt %)/Al <sub>2</sub> O <sub>3</sub>         | 43                 | 13                 | 70    | 78                 | 86                 |
| PtSn(0.5 wt %)/Al <sub>2</sub> O <sub>3</sub>         | 38                 | 16                 | 58    | 83                 | 90                 |
| Pt/Al <sub>2</sub> O <sub>3</sub> -Na                 | 31                 | 16                 | 48    | 79                 | 81                 |
| PtSn(0.3 wt %)/Al <sub>2</sub> O <sub>3</sub> -Na (C) | 34                 | 19                 | 44    | 96                 | 97                 |
| PtSn(0.5 wt %)/Al <sub>2</sub> O <sub>3</sub> -Na (C) | 28                 | 15                 | 46    | 91                 | 93                 |
| PtSn(0.3 wt %)/Al <sub>2</sub> O <sub>3</sub> -Na(SI) | 31                 | 21                 | 32    | 97                 | 98                 |
| PtSn(0.5 wt %)/Al <sub>2</sub> O <sub>3</sub> -Na(SI) | 34                 | 19                 | 44    | 96                 | 97                 |

dehydrogenation reaction with respect to the carbon deposition and its relationship with the *n*-butane conversion, the catalyst deactivation and the selectivity to different products.

Figure 5 shows the effect of the injection of the successive pulses on the selectivity to the different butenes, while Fig. 6 displays the influence on the carbon retention. The carbon retention was calculated by a carbon balance between the inlet and the exit of the reactor.

From data shown in Figs. 5 and 6, the first steps of the dehydrogenation of *n*-butane can be studied and this will be useful for a better understanding of the results in the continuous reaction system. At the first stages of the reaction, the monometallic Pt/Al<sub>2</sub>O<sub>3</sub> catalyst displays a practically negligible selectivity to all butenes (Fig. 5), and hence a total hydrogenolytic selectivity (forming exclusively methane). As the number of pulses increases, the selectivity to all butenes also increases, with the consequent decrease of the hydrogenolytic selectivity. This effect is accompanied by an important carbon retention (or coke deposition) during the first injected pulses. Besides, it can be observed that the carbon deposition decreases with the number of pulses

**Fig. 5** Selectivity to all butenes as a function of the injected butane pulses for Pt/Al<sub>2</sub>O<sub>3</sub> and PtSn/Al<sub>2</sub>O<sub>3</sub> catalysts prepared by successive impregnation**Fig. 6** Values of carbon retention as a function of the injected butane pulses for Pt/Al<sub>2</sub>O<sub>3</sub> and PtSn/Al<sub>2</sub>O<sub>3</sub> catalysts prepared by successive impregnation

(Fig. 6). The monometallic catalyst is very active and it has a lot of hydrogenolytic sites since during the first butane pulses, an important hydrogenolysis or C–C bonds breaking and a large carbon deposition is produced on the surface of Pt/Al<sub>2</sub>O<sub>3</sub> catalyst. It must be noted that similar type of sites would be required for both hydrogenolysis and coke formation reactions. The carbon formation would produce a selective poisoning of these hydrogenolytic sites, thus decreasing the selectivity to methane and increasing the selectivity to the different butenes.

On the other hand, the bimetallic PtSn/Al<sub>2</sub>O<sub>3</sub> catalysts display a selectivity to all butenes higher than that of the monometallic sample. It can be pointed out that this selectivity also increases with the addition of successive pulses (Fig. 5), and the carbon retention is lower than that of the monometallic catalyst (Fig. 6). These differences with the monometallic sample are more pronounced in the bimetallic sample with the highest tin content. In this sense Figs. 5 and 6 show that the catalysts with higher tin contents (0.5 wt%) display higher selectivities to butenes (about 50% for pulse number 20) and lower coke deposition than the sample with 0.3 wt% Sn.

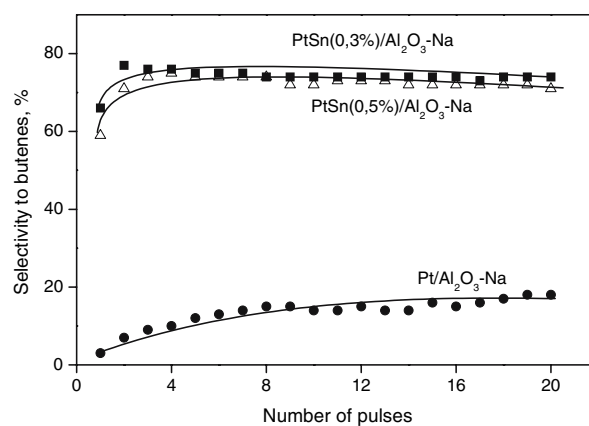
In consequence, these results indicate that the Sn addition to Pt produces a decrease of the hydrogenolytic capacity of the active metal (in agreement with the CP hydrogenolysis results) and it also decreases the coke deposition. The results of carbon retention obtained in pulse experiments indicate that the catalyst deactivation in the continuous flow system would be due to a pronounced coke deposition during the first steps of the reaction. The bimetallic catalysts deactivate in a lower degree because coke is deposited in a lower extension than in the monometallic one. The increase of the selectivity to all butenes in the bimetallic catalysts, would be associated to the presence of a modified metallic phase.

Table 4 (continuous flow experiments) also shows that Na addition to Pt/Al<sub>2</sub>O<sub>3</sub> catalyst decreases the initial conversion ( $X_0$ ) and the deactivation parameter (D) along the reaction time. Besides, the selectivity to butenes is increased up to 80% due to a marked decrease of the hydrogenolytic capacity of the Al<sub>2</sub>O<sub>3</sub>-Na.

Four bimetallic PtSn catalysts with two Sn concentrations (0.3 and 0.5 wt%) prepared by co-impregnation and successive impregnation of Al<sub>2</sub>O<sub>3</sub>-Na (0.5 wt%) were evaluated in the *n*-butane dehydrogenation in the continuous flow reactor and the results are displayed in Table 4. The initial conversions of bimetallic catalysts supported on Al<sub>2</sub>O<sub>3</sub>-Na are similar to that of the monometallic Pt/Al<sub>2</sub>O<sub>3</sub>-Na catalysts, while the deactivation parameter D slightly decreases and the dehydrogenating selectivity sharply increases up to of 93–98%. These results show the excellent performances of bimetallic catalysts supported on Na-doped alumina in the *n*-butane dehydrogenation.

Taking into account the good catalytic performance of PtSn/Al<sub>2</sub>O<sub>3</sub>-Na catalyst, the behavior of the samples during the initial stages of the reaction was evaluated by means of *n*-butane pulse equipment. In this way, Fig. 7 shows the influence of the injected *n*-butane pulses on the selectivity to all butenes for PtSn/Al<sub>2</sub>O<sub>3</sub>-Na catalysts compared with the behavior of a monometallic Pt/Al<sub>2</sub>O<sub>3</sub>-Na sample. It is also observed that the monometallic catalyst maintains a very low dehydrogenating selectivity (lower than 20%) whereas, the bimetallic samples show a high selectivity to all butenes that increases from 60% (first pulse) up to 75% for the twentieth pulse. This indicates that the tin addition to Pt/Al<sub>2</sub>O<sub>3</sub>-Na (0.5 wt%) catalyst inhibits the hydrogenolytic reactions and hence increases the dehydrogenation towards the different butenes.

With respect to the carbon retention during the initial steps of the reaction (Fig. 8), bimetallic catalysts supported on Na doped alumina (both C and SI), show lower carbon retention than the monometallic catalyst supported on the Na doped support along the different injected butane pulses. This means that during the initial moments of the reaction, the tin addition to Pt/Al<sub>2</sub>O<sub>3</sub>-Na



**Fig. 7** Selectivity to butenes as a function of the butane pulses injected at 530 °C on the mono and bimetallic catalysts prepared by successive impregnation supported on Na-doped alumina

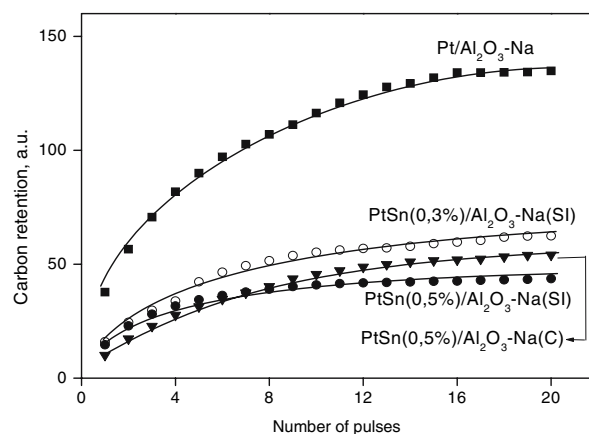


**Fig. 8** Values of carbon retention as a function of the butane pulses injected at 530 °C on mono and bimetallic catalysts (prepared by successive impregnation and co-impregnation) supported on Na(0.5 wt%)-doped alumina

catalyst inhibits the coke deposition reactions and the hydrogenolytic ones.

By comparing Fig. 8 with Fig. 6, it must be noted that the monometallic catalyst supported on Na-doped alumina, shows lower carbon retention than both the Na-undoped monometallic sample and the bimetallic PtSn catalysts supported on alumina, therefore, Na decreases the coke deposition since it poisons the acidic sites of the alumina that cause the carbon formation.

## 4 Conclusions

The light paraffin dehydrogenation into olefins on supported metallic catalysts is accompanied by undesirable reactions that produce light products and carbon deposition. The formation of light products (methane, ethane,

ethylene, propane, etc.) on bifunctional catalysts could take place through different mechanisms: (a) monofunctional mechanisms consisted in hydrogenolysis on the metal and hydrocracking on the acidic function, and (b) bifunctional mechanism in which the olefin formed on the metal can migrate to the acidic sites of the support where it is cracked. In our case, the low acidity of  $\gamma$ -Al<sub>2</sub>O<sub>3</sub> is not enough to promote the direct cracking of *n*-butane. Hence, this route would not be important in the formation of light products.

The results above mentioned show that the Sn addition to Pt produces important modifications in the behavior of these catalysts in the butane dehydrogenation reaction. In this sense, the use of different impregnation sequences does not produce important changes in the performance of the bimetallic catalysts. Results show that Sn addition to Pt/Al<sub>2</sub>O<sub>3</sub> catalyst decreases the catalyst deactivation. Besides, the selectivity to all butenes is markedly increased from 55% for the Pt/Al<sub>2</sub>O<sub>3</sub> catalyst (at 2 h reaction time) up to values of 85–90% for the bimetallic catalysts (at the same reaction time).

The different behavior of PtSn/Al<sub>2</sub>O<sub>3</sub> bimetallic catalysts in the butane dehydrogenation with respect to the monometallic sample is related to strong structural modifications produced by the addition of the Group IV-A metal to Pt, such as it can be corroborated from the characterization results. In fact, evidences obtained from the shapes of the TPR profiles, XPS results and from the marked increase of the activation energy values of the CHD reaction, indicate the presence of strong electronic interactions between both metals. Besides CP hydrogenolysis results would indicate that Sn not only modifies electronically but also geometrically the Pt. Thus the Sn appears to be placed in the vicinities of the active metal (Pt) with the consequent elimination of the hydrogenolytic and coke formation ensembles. In this way, there would be particles of PtSn alloys (probably with different compositions) together with Pt<sup>0</sup> species and oxidized Sn particles, the last ones stabilized on the support. In this way the active centers of the metallic phase would be diluted by the other species, thus leading to a phase with a high dehydrogenating selectivity, and very low hydrogenolytic and coke formation capacities. Finally, the modification of the metallic phase by Sn addition could also produce a decrease of the adsorption strength of the coke precursors, such as Bocanegra et al. observed for PtSn/ZnAl<sub>2</sub>O<sub>4</sub> catalysts [36]. In this sense the tin addition to Pt could decrease the adsorption of unsaturated molecules on the metal, thus favoring their desorption to the gas phase, once they were formed. In this way, more olefins would be produced and hence lower carbon amounts would be deposited on the metal.

Taking into account the different results of metallic and acidic phase characterization and the evaluation in *n*-butane

dehydrogenation, there is a complex effect produced by the Na addition to PtSn/Al<sub>2</sub>O<sub>3</sub> catalysts. The influence of Na on the alumina is directly related to the poisoning effect on the acidic sites of the support, such as can be seen from isopropanol dehydration results, but this is not the only effect, since important modifications of the characteristics of the metallic phase are also observed. In this sense, TPR results show the presence of strong PtSn interactions, with probable alloy formation, which would be responsible for the decrease of the reaction rate and the increase of the activation energy in CHD. Besides, the experiments of CPH show that the alkali metal addition to bimetallic PtSn/Al<sub>2</sub>O<sub>3</sub> catalysts completely eliminates the hydrogenolytic ensembles and geometrically modifies the metallic phase.

These important modifications in the nature of the metallic function due to the simultaneous incorporation of Na and Sn to Pt/Al<sub>2</sub>O<sub>3</sub> would be responsible for the excellent catalytic performance in the butane dehydrogenation that promotes very good conversions, selectivities to all butenes higher than 95%, and lower deactivation capacity than those corresponding to bimetallic PtSn catalysts supported on undoped alumina. The excellent stability of these bimetallic catalysts supported on Al<sub>2</sub>O<sub>3</sub>-Na would be due to a low carbon formation during the reaction, such as is observed in comparing the carbon retention results during the pulses experiments (Figs. 6 and 8).

**Acknowledgments** Authors thank Dr. F. Coloma (Universidad de Alicante, España) for the XPS measurements and Mr. Miguel Torres for the experimental assistance. Besides, this work was made with the financial support of Universidad Nacional del Litoral, ANPCyT and CONICET Argentina.

## References

1. Castro AA (1993) *Catal Lett* 22:123
2. Yarusov IB, Zatulokina EV, Shitova NV, Belyi AS, Ostrovskii NM (1992) *Catal Today* 13:655
3. Jablonski EL, Castro AA, Scelza OA, de Miguel SR (1999) *Appl Catal A: Gen* 183:189
4. Yu C, Ge Q, Xu H, Li W (2006) *Appl Catal A: Gen* 315:58
5. Epron F, Carnevillier C, Marecot P (2005) *Appl Catal A: Gen* 295:157
6. Padmavathi G, Chaudhuri KK, Rajeshwer D, Sreenivasa Rao G, Krishnamurthy KR, Trivedi PC, Hathi KK, Subramanyam N (2005) *Chem Eng Sc* 60:4119
7. Parera JM, Figoli NS (1995) In: Antos G, Aitani A, Parera JM (eds) *Catalytic naphtha reforming science and technology*. Chapter 3 Marcel Dekker, Inc., New York, pp 45–78
8. Pines H, Haag W (1960) *J Am Chem Soc* 82:2471
9. Jiratová K, Beránek L (1982) *Appl Catal* 2:125
10. García Cortéz G, de Miguel SR, Scelza OA, Castro AA (1992) *J Chem Tech Biotechnol* 53:177
11. Bocanegra S, Castro AA, Guerrero Ruiz A, Scelza OA, de Miguel SR (2006) *Chem Eng J* 118:161
12. de Miguel SR, Scelza OA, Castro AA, Soria J (1994) *Top Catal* 1:87
13. Mross WD (1983) *Catal Rev Sci Eng* 25:591

14. Park YH, Price GL (1991) *J Chem Soc Chem Commun* 1188
15. Park YH, Price GL (1992) *Ind Eng Chem Res* 31:469
16. Rodriguez D, Sanchez J, Arteaga G (2005) *J Mol Catal A: Chem* 228:309
17. Vernoux P, Leinekugel-Le-Cocq A-Y, Gaillard F (2003) *J Catal* 219:247
18. Cinneide D, Clarke JKA (1972) *Catal Rev* 7:233
19. Boudart M (1969) *Adv Catal* 20:153
20. Lieske H, Lietz G, Spindler H, Völter J (1983) *J Catal* 81:8
21. Lietz G, Lieske H, Spindler H, Hanke W, Völter J (1983) *J Catal* 81:17
22. Padró CL, de Miguel SR, Castro AA, Scelza OA (1997) *Stud Surf Sci Catal* 111:191
23. Siri G, Ramallo-Lopez J, Casella M, Fierro JLG, Requejo F, Ferretti O (2005) *Appl Catal A: Gen* 278:239
24. Kappenstein C, Saouabe M, Guerin M, Marecot P, Uszkurat I, Paal Z (1995) *Catal Lett* 31:9
25. McNicol B (1987) *J Catal* 46:438
26. Wastaff N, Prins R (1979) *J Catal* 59:434
27. Lee C-H, Chen Y-W (1997) *Ind Eng Chem Res* 36:1498
28. Rodriguez D, Sanchez J, Arteaga G (2005) *J Mol Catal A: Chem* 228:309
29. Serrano-Ruiz JC, Huber GW, Sanchez-Castillo MA, Dumesic J, Rodríguez-Reinoso F, Sepúlveda-Escribano A (2006) *J Catal* 241:378
30. Huidobro A, Sepúlveda-Escribano A, Rodríguez-Reinoso F (2002) *J Catal* 212:94
31. Merlen E, Beccat P, Bertolini JC, Delichere P, Zanier N, Didillon B (1996) *J Catal* 159:178
32. Homs N, Llorca J, Riera M, Jolis J, Fierro JLG, Sales J, Ramírez de la Piscina P (2003) *J Mol Catal A: Chem* 200:251
33. Llorca J, Ramírez de la Piscina P, Fierro JLG, Sales J, Homs N (1997) *J Mol Catal A: Chem* 118:101
34. Wagner CD, Riggs WM, Davis LE (1993) Moulder JF handbook of X-ray photoelectron spectroscopy
35. Stencel JM, Goodman J, Davis BH (1988) In: Proceedings of the 9th international congress on catalysis, Calgary, Canada, p 1291
36. Bocanegra S, Guerrero-Ruiz A, de Miguel S, Scelza O (2004) *Appl Catal A: Gen* 277:11
37. Balakrishnan K, Schwank J (1991) *J Catal* 127:287
38. Vilella IMJ, de Miguel SR, Salinas-Martínez de Lecea C, Linares-Solano A, Scelza OA (2005) *Appl Catal A: Gen* 281:247